Macromolecules
ARTICLE

Macromolecules **2009**, *42*, 4853–4857 **4853**
DOI: 10.1021/ma900462a

Probing the Elemental Environment around the Free Volume in Polymers with Positron Annihilation Age−Momentum Correlation Spectroscopy

K. Sato,*,† H. Murakami,† K. Ito,‡ K. Hirata,‡ and Y. Kobayashi‡

†*Department of Environmental Sciences, Tokyo Gakugei University, 4-1-1 Koganei, Tokyo 184-8501, Japan, and* ‡*National Institute of Advanced Industrial Science and Technology (AIST), Tsukuba, Ibaraki 305-8565, Japan*

Received March 3, 2009; Revised Manuscript Received April 15, 2009

ABSTRACT: Time-resolved momentum distributions of positron−electron annihilation photons were investigated for various polymers by means of positron age−momentum correlation (AMOC) spectroscopy. The momentum distribution exclusively associated with orthopositronium (o-Ps) pick-off annihilation is found to be element-specific and can sensitively probe different light atoms such as C, O, F, and Si that constitute the surface of nanometer-sized free volumes. It is demonstrated that the chemical environment around free volumes in polymers for practical use can be probed by positron annihilation AMOC spectroscopy.

1. Introduction

Nanometer-sized open spaces (free volumes) in polymers play an important role in transport phenomena such as gas permeation and ionic conduction.[1,2] Recent advances in polymer nanoprocessing technology have led to increased interest in the detailed structures of free volumes in relation to ionic diffusion through a particular polymer chain,[3] highly selective gas separation by finely controlled structures, etc.[4,5]

Positron annihilation lifetime spectroscopy is of great usefulness for the study of free volumes in polymers.[6] A fraction of energetic positrons injected into polymers forms the bound state with an electron, positronium (Ps).[7] Singlet parapositronium (p-Ps) with the spins of the positron and electron antiparallel and triplet orthopositronium (o-Ps) with parallel spins are formed at a ratio of 1:3. Hence, three states of positrons, p-Ps, o-Ps, and free positrons, exist in polymers. The annihilation of p-Ps results in the emission of two γ-ray photons of 511 keV with lifetime ~125 ps. Free positrons are trapped by negatively charged parts such as polar elements and annihilated into two photons with lifetime ~450 ps.[8−10] The positron in o-Ps undergoes two-photon annihilation with one of the bound electrons with a lifetime of a few nanoseconds after localization in free volumes.[11,12] The last process is known as o-Ps pick-off annihilation and provides information on the free volume size through its lifetime $\tau_{o\text{-}Ps}$ based on the Tao−Eldrup model:

$$\tau_{o-Ps} = 0.5\left[1 - \frac{R}{R_0} + \frac{1}{2\pi}\sin\left(\frac{2\pi R}{R_0}\right)\right]^{-1} \quad (1)$$

where $R_0 = R + \Delta R$, and $\Delta R = 0.166$ nm is the thickness of the homogeneous electron layer in which the positron in o-Ps annihilates.[13,14]

Positron annihilation momentum spectroscopy is based on the principle that if the positron−electron annihilation accompanies a longitudinal momentum p, the resulting annihilation γ-rays are Doppler-shifted from m_0c^2 by $\pm cp/2$.[15] Here, m_0 and c are the electron rest mass and velocity of light, respectively. Measurements of the Doppler shifts by γ-ray energy spectroscopy make it possible to obtain information on the momentum distribution of the positron−electron annihilation pairs. The momentum of p-Ps annihilation has a narrow distribution because p-Ps self-annihilates after losing the initial energy. In contrast to that, the momentum distribution of free positrons is significantly broadened due to the large momenta of electrons participating in the annihilation. The momentum distribution of o-Ps is also broadened because the pick-off annihilation is influenced by electrons bound to the surrounding molecules. In most cases, the momentum distribution is conveniently evaluated by the line-shape S parameter, which is defined as the ratio of integrated counts typically over ±1 keV from the center of the 511 keV peak to the total integrated counts approximately over ±5 keV from the center of the 511 keV peak after the background is properly subtracted, as illustrated in Figure 1. Broadening of the spectrum decreases the S parameter, while narrowing of the spectrum increases the S parameter. The S parameter of p-Ps self-annihilation is remarkably higher than those of the positron and o-Ps due to its narrower momentum distribution.

In polymers, p-Ps, free positrons, and o-Ps all contribute to the overall momentum distribution of the annihilation pairs. In order to obtain information specific to the free volume, the momentum distribution of o-Ps pick-off annihilation has to be extracted. In this work, we show that time resolving the annihilation photons with positron age−momentum correlation (AMOC) spectroscopy provides the element-specific momentum distribution exclusively associated with o-Ps, which is sensitive to the chemical environment around free volumes in polymers.

2. Experiment

2.1. Samples. Polystyrene (PS), high-density polyethylene (HDPE), polypropylene (PP), polycarbonate (PC), poly(ester carbonate) (PEC), poly(ether sulfone) (PES), ethylene−tetrafluoroethylene copolymer (ETFE), poly(tetrafluoroethylene) (PTFE), and poly(vinyl fluoride) (PVF) were studied in this work (see Table 1). Hereafter, C-containing polymers (PS, HDPE, and PP), O-containing polymers (PC, PEC, and PES), and F-containing polymers (ETFE and PTFE) are

*To whom correspondence should be addressed: Tel: +81-42-329-7546; E-mail: sato-k@u-gakugei.ac.jp.

Published on Web 05/04/2009

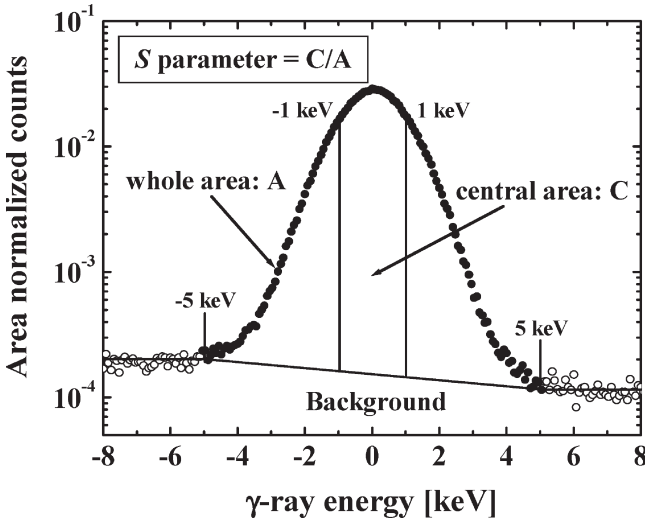

Figure 1. Schematic diagram of the Doppler broadening spectrum and definition of the *S* parameter.

Table 1. Polymers Studied in the Present Work

polymer	ID
C-containing polymers	
polystyrene	PS
high-density polyethylene	HDPE
polypropylene	PP
O-containing polymers	
polycarbonate	PC
poly(ester carbonate)	PEC
poly(ether sulfone)	PES
F-containing polymers	
ethylene−tetrafluoroethylene copolymer	ETFE
poly(tetrafluoroethylene)	PTFE
poly(vinyl fluoride)	PVF

referred to C, O, and F groups, respectively. In addition to the above polymers, undoped and Cs-doped amorphous SiO_2 were studied.

2.2. Positron Age−Momentum Correlation (AMOC) Spectroscopy. Figure 2 shows a schematic diagram of our AMOC spectrometer. In AMOC spectroscopy, the Doppler broadening data correlated with positron lifetimes are recorded. The 1.27 MeV positron birth γ-ray from a ^{22}Na source sealed in a thin foil of Kapton and one of the 511 keV γ-rays emitted as a result of positron annihilation in the samples are detected by BaF_2 scintillators with 2 in. diameter × 1 in. thickness coupled with photomultiplier tubes (PMT1 and PMT2). PMT1 and PMT2 are squarely aligned to each other. The source is mounted in a sample−source−sample sandwich. The 1.27 MeV positron birth γ-ray and 511 keV annihilation γ-ray are energy-selected by constant-fraction-differential discriminators (CFDD1 and CFDD2), and the timing pulse from CFDD1 is delayed by a time-delay module (DELAY). Subsequently, a time-to-amplitude converter (TAC) produces an analogue output, whose height is proportional to the time interval between 1.27 MeV and 511 keV γ-rays. Analogue signals from TAC are transferred to a two-parameter multichannel analyzer (2D-MCA) with a built-in analog-to-digital-convertor (ADC).

For the simultaneous measurement of the energy of the second annihilation γ-rays, a high-purity Ge detector is placed collinearly to PMT2. Analogue pulses from the Ge detector are transferred to the 2D-MCA with the built-in ADC through an amplifier (AMP). A pair of correlated digital outputs of positron lifetime and Doppler broadening data within a certain coincident time is stored in a random access memory, controlled by a personal computer (PC).

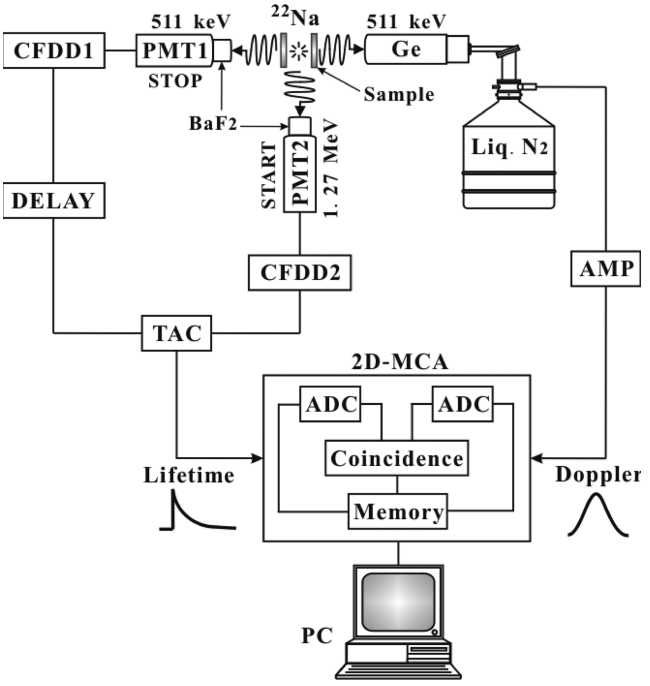

Figure 2. Schematic diagram of the positron age−momentum correlation (AMOC) system.

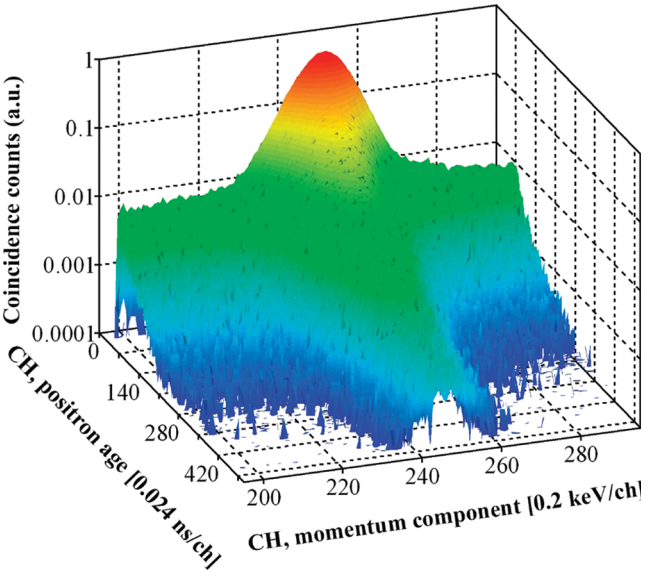

Figure 3. Positron age−momentum correlation (AMOC) spectrum observed for amorphous SiO_2. The coincidence counts are plotted in logarithmic scale as functions of both the positron age and momentum component of annihilation photons.

Figure 3 shows a typical AMOC spectrum for amorphous SiO_2, in which coincidence counts are plotted in logarithmic scale as functions of both the positron age and momentum of the annihilation pairs. Positron-age-dependent Doppler broadening spectra were analyzed as the *S* parameter ($S(t)$). For AMOC spectroscopy, the *S* parameter was defined as the ratio of integrated counts over ±1 keV from the center of 511 keV peak to the total integrated counts over ±5 keV from the center of 511 keV peak after subtracting the background. For clarity of presentation, three neighboring point averaging smoothing was applied.

2.3. Positron Lifetime and Momentum Spectroscopy. Positron annihilation lifetime and momentum measurements were separately conducted in addition to AMOC spectroscopy.

Positron lifetime measurements were performed with a conventional fast−fast coincident system with a time resolution of ~230 ps. Positron lifetime spectra were numerically analyzed using the POSITRONFIT code.[16] The longest-lived component with $\tau_{o\text{-}Ps}$ and its relative intensity $I_{o\text{-}Ps}$ was attributed to o-Ps pick-off annihilation. Lifetime distributions were obtained by using the MELT code.[17] Distributions of free volume sizes (R) were evaluated from the distributions of o-Ps lifetimes based on the Tao-Eldrup model.[13,14]

Momentum distributions of annihilation photons were obtained by coincident measurements of Doppler broadened positron annihilation γ-rays. The measurements were performed by recording the energies of two annihilation quanta E_1 and E_2 with a collinear setup of two high-purity Ge-detectors. The Doppler broadening spectra were obtained by cutting the E_1 and E_2 spectra along the energy conservation line $E_1 + E_2 = 1022 \pm 1$ keV, taking into account the annihilation events within a strip of ±1.6 keV. A cut along the diagonal was then analyzed by taking the S parameter, which was determined for momentum spectroscopy as the ratio of integrated counts over ±0.6 keV from the center of 511 keV peak to the total integrated counts over ±5 keV from the center of 511 keV peak after subtracting the background and the source component of Kapton (~8%).

3. Results

Figure 4a shows the S parameters obtained by AMOC spectroscopy as a function of positron age ($S(t)$) for undoped and Cs-doped amorphous SiO_2. The S parameters indicate high values around $t = 0$. They rapidly decrease with increasing positron age up to 0.5 ns and then level off above 2.0 ns. In Figure 4a, the average lifetimes of p-Ps, free positrons, and o-Ps are indicated with thick arrows pointing to the corresponding positron ages of the horizontal axis. At younger positron age, p-Ps, o-Ps, and positrons all contribute to the momentum distributions of positron−electron annihilation. Around $t = 0$ ns, high values of S parameters are observed due to the narrow momentum distribution of p-Ps self-annihilation. At the positron age above 0.4 ns, more than 90% of the shortest-lived p-Ps has already disappeared. Above 1.2 ns, the positrons have mostly disappeared as well, and as a consequence, o-Ps dominantly contributes to the momentum distribution. The saturated values of $S(t)$ at older positron age thus reflect the momentum distributions of o-Ps pick-off annihilation.

The saturated values of $S(t)$ are significantly higher for Cs-doped amorphous SiO_2 than for the undoped one. This demonstrates narrowing of the momentum distribution of o-Ps pick-off annihilation in the former. Upon Cs doping, free volumes in amorphous SiO_2 mostly surrounded by O atoms[18] get partially occupied by Cs atoms, which is seen in the variation of the free-volume size distribution obtained from $\tau_{o\text{-}Ps}$ determined by conventional lifetime spectroscopy with the Tao−Eldrup model (see Figure 4b). Higher S parameters after Cs doping in the older positron age region indicate the narrower momentum distribution of o-Ps pick-off annihilation in free volumes partially surrounded by Cs atoms. S parameters at older positron age are thus sensitive to the chemical environment around free volumes.

Figure 5 shows S parameters obtained by AMOC spectroscopy as a function of positron age for C-containing polymers (PS, HDPE, and PP), O-containing polymers (PC, PEC, and PES), and F-containing polymers (ETFE and PTFE). Tendencies of S parameters decreasing with positron age are similar to Figure 4a, except dips around a positron age of 0.6 ns for the O and F groups. This is due to positron trapping on polar elements as, e.g., O and F atoms and annihilation with the electrons of higher momenta.[8−10] The S parameters are very similar to each other for the C and O groups, whereas they are consistently lower for the F group. Thus, the chemical environment around free volumes may be similar for the C and O groups but different for the F group. In the C and O groups, most constituents are C atoms, whereas more than 60% of constituents are F atoms in the F group. Hence, F, C and O groups are distinguishable by o-Ps, and the bulk composition of polymers is reflected in the chemical environment around free volumes probed by AMOC spectroscopy.

Figure 6a shows a comparison of AMOC data between amorphous SiO_2 and the O group polymers (PC, PEC, and PES). At older positron age, S parameters are remarkably lower for amorphous SiO_2 than the O group polymers, indicating broadening of the momentum distribution of o-Ps pick-off annihilation for the former. In Ps-forming materials, the overall S parameter measured by momentum spectroscopy commonly increases with increasing Ps formation following the equation

$$S = (1-f)S_{e+} + fS_{Ps} \quad (2)$$

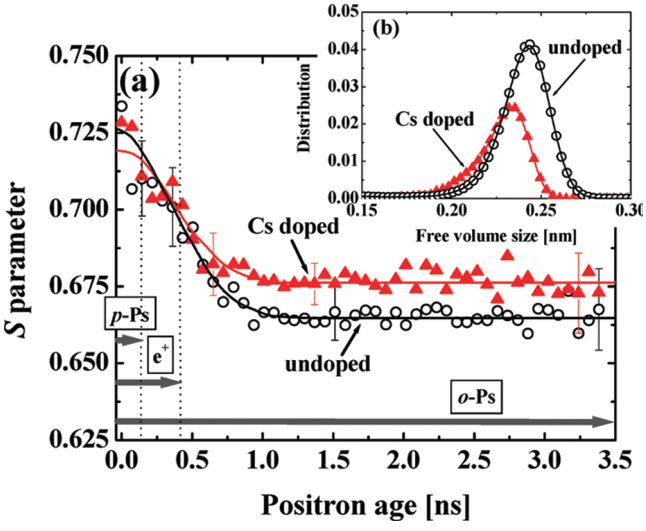

Figure 4. (a) Positron age dependence of the $S(t)$ parameters obtained by AMOC spectroscopy for undoped (open circles) and Cs-doped (solid triangles) amorphous SiO_2. Solid lines are drawn for guiding the eye. Time scales of lifetimes of p-Ps, free positron, and o-Ps are illustrated with thick arrows. (b) Free-volume size distributions for undoped (open circles) and Cs-doped (solid triangles) amorphous SiO_2.

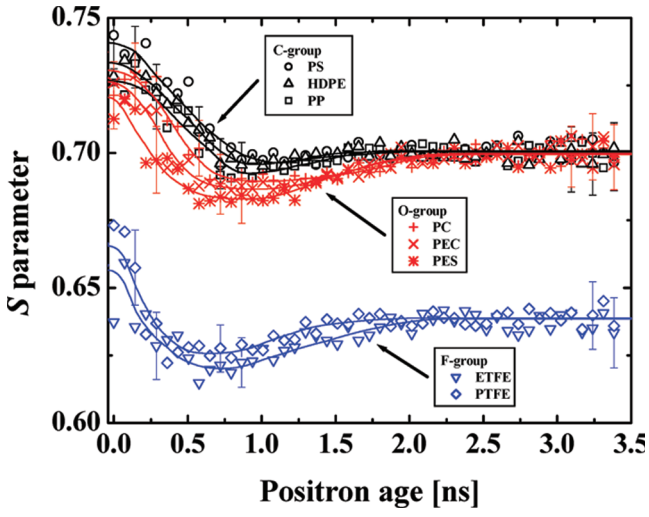

Figure 5. Positron age dependence of the $S(t)$ parameters obtained by AMOC spectroscopy for PS (open circles), HDPE (open triangles), PP (open squares), PC (horizontal crosses), PEC (diagonal crosses), PES (stars), ETFE (open inverse triangles), and PTFE (diamonds). Solid lines are drawn for guiding the eye.

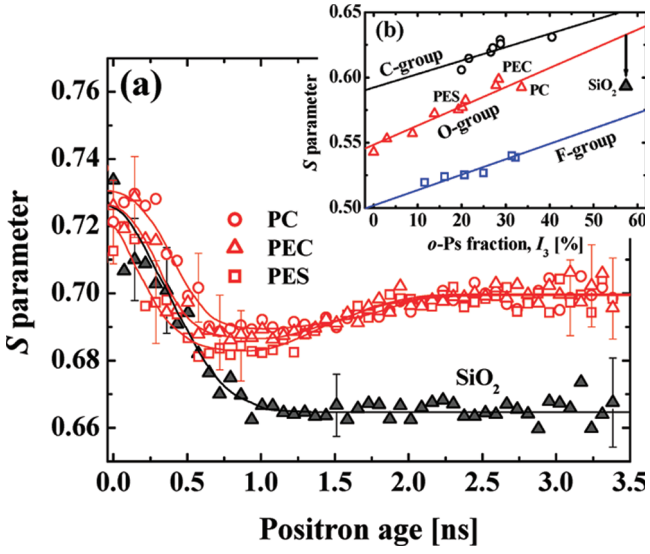

Figure 6. (a) Positron age dependence of the $S(t)$ parameters obtained by AMOC spectroscopy for PC (open circles), PEC (open triangles), PES (open squares), and amorphous SiO_2 (solid triangles). Solid lines are drawn for guiding the eye. (b) Correlation between the overall S parameter and o-Ps fraction for C (open circles), O (open triangles), and F (open squares) containing polymers (ref 19). Solid lines are results of the least-squares fits for respective polymer groups. The data for amorphous SiO_2 are newly plotted with a solid triangle. S parameters in (a) and (b) are not comparable to each other due to different energy windows, signal-to-noise ratios, energy resolutions, and so on.

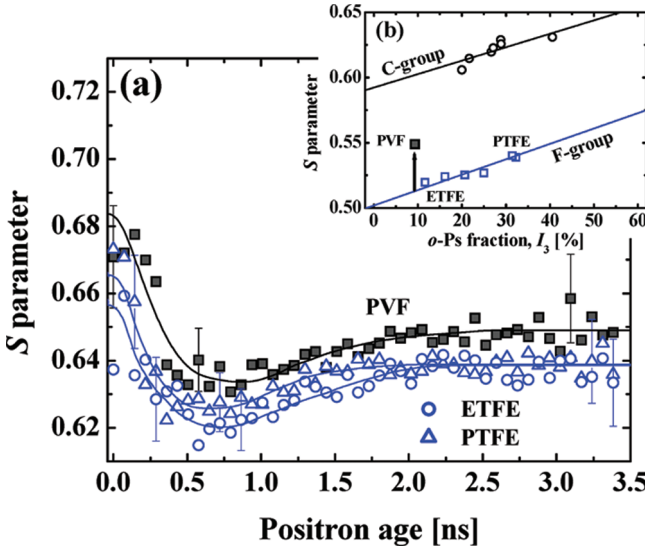

Figure 7. (a) Positron age dependence of the $S(t)$ parameters obtained by AMOC spectroscopy for ETFE (open circles), PTFE (open triangles), and PVF (solid squares). Solid lines are drawn for guiding the eye. (b) Correlation between the overall S parameter and o-Ps fraction for C (open circles) and F (open squares) containing polymers (ref 19). Solid lines are results of the least-squares fits for respective polymer groups. The data for PVF is newly plotted with a solid square. S parameters in (a) and (b) are not comparable to each other due to different energy windows, signal-to-noise ratios, energy resolutions, and so on.

where S_{e+}, S_{Ps}, and f are the S parameters individually contributed from the e^+, Ps, and the fraction of Ps formation, respectively. Since p-Ps and o-Ps are formed at a ratio of 1:3 and $f = (4/3)I_{o\text{-}Ps}$, eq 2 is rewritten as

$$S = S_{e+} + \frac{4}{3}\Delta S I_{o-Ps} \tag{3}$$

with

$$\Delta S = \frac{1}{4}S_{p-Ps} + \frac{3}{4}S_{o-Ps} - S_{e+} \tag{4}$$

where $S_{p\text{-}Ps}$ and $S_{o\text{-}Ps}$ are the contributions from p-Ps and o-Ps, respectively, and $I_{o\text{-}Ps}$ is the o-Ps yield determined as the relative intensity of the longest-lived component by conventional lifetime spectroscopy. Under the condition of common S_{e+} and S_{Ps}, the overall S parameter obtained by momentum spectroscopy linearly increases with increasing $I_{o\text{-}Ps}$ as shown by the different lines for the three polymer groups in Figure 6b.[9,19,20] The data of amorphous SiO_2 in the $S-I_3$ correlation are largely deviated from those of the O group. As can be seen from eqs 3 and 4, lowering of $S_{o\text{-}Ps}$ makes gradient $(4/3)\Delta S$ less steep, thus causing a downward deviation from the correlation of the O group. Broadening of the momentum distribution of o-Ps pick-off annihilation for amorphous SiO_2 probed by AMOC spectroscopy is therefore consistent with the $S-I_3$ correlation. As demonstrated above, the bulk composition of polymers is reflected in the chemical environment around free volumes. It is thus C-rich for O-containing polymers, which consist mostly of C atoms (see Figure 5). In contrast to that, O-enriched free volumes are present in amorphous SiO_2,[18] and the momentum distribution of o-Ps pick-off annihilation is broadened for amorphous SiO_2 with more O atoms located around free volumes.

Figure 7 shows the S parameters obtained by AMOC spectroscopy as a function of positron age for PVF, ETFE, and PTFE. The S parameters at older positron age for PVF are significantly higher than the other two F-containing polymers, indicating a narrower momentum distribution of o-Ps pick-off annihilation. We note the data of PVF largely deviated from the $S-I_3$ correlation of the F group (see Figure 7b). It is obvious from eq 2 that the narrowing of o-Ps annihilation increases the overall S parameter, leading to upward deviation from the correlation of the F group. In light of dramatic broadening of o-Ps pick-off annihilation with electrons of F atoms as revealed in Figure 5, free volumes in PVF are supposed to be surrounded by less F atoms than the other F-containing polymers. This is fully supported by the chemical structure of PVF, where the number of F atoms is much less than the other F-containing polymers.

4. Discussion

By time-resolving positron−electron annihilation photons with positron age−momentum correlation (AMOC) spectroscopy, momentum distributions exclusively associated with orthopositronium (o-Ps) pick-off annihilation can be extracted for various polymers. The momentum distribution of o-Ps pick-off annihilation significantly changes after free volumes get partially surrounded by Cs atoms for amorphous SiO_2. Furthermore, the momentum distribution of o-Ps depends on the composition of C-, O-, and F-containing polymers, where the bulk composition is reflected in surfaces of free volumes. Our experimental results demonstrate that o-Ps pick-off annihilation differentiates elements on free volume surfaces.

Fractional numbers f_F of F atoms in the F-containing polymers are 0.67 (tetrafluoroethylene−perfluorovinyl ether copolymer, tetrafluoroethylene perfluoropropylvinyl ether copolymer, and PTFE), 0.33 (ETFE), 0.25 (poly(vinylidene fluoride)), and 0.17 (PVF). According to Bamford et al.,[21] S parameters deduced from Doppler broadening spectra of F- and O-containing polymers after subtraction of the narrowest p-Ps component decrease with increasing f_F up to ~0.5, which may result from the combined effect of o-Ps pick-off annihilation and positron trapping on polar elements. The effect of positron trapping on polar F atoms is clearly visible in the dips observed around the

positron age of 0.6 ns (see Figure 7). The present results indicate that o-Ps can differentiate the chemical environment around free volumes with $f_F < 0.17$. As for O atoms, o-Ps distinctly differentiates the chemical environment around free volumes with a higher fractional number of O atoms f_O for amorphous SiO_2 (0.67) from the O-containing polymers (~0.3). Therefore, the free volume analysis with o-Ps pick-off annihilation photons by AMOC spectroscopy may be effective for F- and O-containing polymers approximately in the composition range $f_F < 0.17$ and $f_O > 0.67$, respectively.

The evaluation of the free-volume size from the o-Ps lifetime has been the only subject of nanospace characterization of polymers with positrons.[13,14,22−25] It is, in this sense, highly beneficial that one can probe different elements like C, O, F, and Si constituting the surface of nanospaces by AMOC spectroscopy. In nanoprocessing of functional polymers, molecularly designed nanospaces with the chemical environment specific to target elements or ions are required.[26] The chemical analysis of free volume by the present technique will be a powerful tool for the study of novel functional polymers.

5. Conclusion

By time-resolving positron−electron annihilation photons with positron age−momentum correlation (AMOC) spectroscopy, one can extract momentum distributions exclusively associated with orthopositronium (o-Ps) pick-off annihilation in various polymers. It is found that the momentum distribution is able to probe different light atoms on the surface of nanometer-sized free volumes, and AMOC spectroscopy can be applied to the analyses of chemical environment around free volumes in polymers for practical use. Chemical environment analysis by AMOC spectroscopy combined with hole-size measurements by positron lifetime spectroscopy will be highly useful for the characterization and fine control of free volumes in polymers.

Acknowledgment. This work was partially supported by Grants-in-Aid for Scientific Research from the Ministry of Education, Science, Sports and Culture of Japan (Grants 18840016, 18560651, and 20740173), the New Energy and Industrial Technology Development Organization (NEDO), and Asahi Glass Foundation.

References and Notes

(1) Obeidi, Sh.; Stolwijk, N. A.; Pass, S. J. *Macromolecules* **2005**, *38*, 10750.
(2) Ma, W.; Andersson, A.; He, J.; Maurer, F. H. J. *Macromolecules* **2008**, *41*, 5307.
(3) Borodin, O.; Smith, G. D.; Douglas, R. *J. Phys. Chem. B* **2003**, *107*, 6824.
(4) Park, H. B.; Jung, C. H.; Lee, Y. M.; Hill, A. J.; Pas, S. J.; Mudie, S. T.; Wagner, E. V.; Freeman, B. D.; Cookson, D. J. *Science* **2007**, *318*, 254.
(5) Sterescu, D. M.; Stamatialis, D. F.; Mendes, E.; Kruse, J.; Rätzke, K.; Faupel, F.; Wessling, M. *Macromolecules* **2007**, *40*, 5400.
(6) *Positron Solid State Physics*; Brandt, W., Dupasquier, A., Eds.; North-Holland: Amsterdam, 1983.
(7) Algers, J.; Sperr, P.; Egger, W.; Kögel, G.; Maurer, F. H. *J. Phys. Rev. B* **2003**, *67*, 125404.
(8) Nagai, Y.; Nonaka, T.; Hasegawa, M.; Kobayashi, Y.; Wang, C. L.; Zheng, W.; Zhang, C. *Phys. Rev. B* **1999**, *60*, 11863.
(9) Ito, K.; Kobayashi, Y.; Nanasawa, A. *Appl. Phys. Lett.* **2003**, *82*, 654.
(10) Kobayashi, Y.; Wang, C. L.; Hirata, K.; Zheng, W.; Zhang, C. *Phys. Rev. B* **1998**, *58*, 5384.
(11) Wästlund, C.; Maurer, F. H. J. *Macromolecules* **1997**, *30*, 5870.
(12) Schmidt, M.; Maurer, F. H. J. *Macromolecules* **2000**, *33*, 3879.
(13) Tao, S. J. *J. Chem. Phys.* **1972**, *56*, 5499.
(14) Eldrup, M.; Lightbody, D.; Sherwood, J. N. *Chem. Phys.* **1981**, *63*, 51.
(15) Mogensen, O. E. *Positron Annihilation in Chemistry*; Springer-Verlag: Berlin, 1995.
(16) Kirkegaard, P.; Eldrup, M. *Comput. Phys. Commun.* **1974**, *7*, 401.
(17) Shukla, A.; Hoffmann, L.; Manuel, A. A.; Peter, M. *Mater. Sci. Forum* **1997**, *255−257*, 233.
(18) Zachariasen, W. H. *J. Am. Chem. Soc.* **1932**, *54*, 3841.
(19) Sato, K.; Ito, K.; Hirata, K.; Yu, R. S.; Kobayashi, Y. *Phys. Rev. B* **2005**, *71*, 012201.
(20) Sato, K.; Shanai, D.; Hotani, Y.; Ougizawa, T.; Ito, K.; Hirata, K.; Kobayashi, Y. *Phys. Rev. Lett.* **2006**, *96*, 228302.
(21) Bamford, D.; Dlubek, G.; Dommet, G.; Höring, S.; Lüpke, T.; Kilburn, D.; Alam, M. A. *Polymer* **2006**, *47*, 3486.
(22) Ito, K.; Nakanishi, H.; Ujihira, Y. *J. Phys. Chem. B* **1999**, *103*, 4555.
(23) Oka, T.; Ito, K.; Muramatsu, M.; Ohdaira, T.; Suzuki, R.; Kobayashi, Y. *J. Phys. Chem. B* **2006**, *110*, 20172.
(24) Oka, T.; Ito, K.; He, C.; Dutriez, C.; Yokoyama, H.; Kobayashi, Y. *J. Phys. Chem. B* **2008**, *112*, 12191.
(25) Mohamed, H. F. M.; Kobayashi, Y.; Kuroda, C. S.; Ohira, A. *J. Phys. Chem. B* **2009**, *113*, 2247.
(26) For example: Maitra, A.; Heuer, A. *Phys. Rev. Lett.* 2007, *98*, 227802.